Energy bands of (100) copper thin films*

K. S. Sohn, D. G. Dempsey, Leonard Kleinman, and Ed Caruthers
Department of Physics, University of Texas, Austin, Texas 78712
(Received 28 August 1975)

We report a tight-binding calculation of the energy bands of a 33-layer (100) copper thin film. Thirty-four parameters for the Hamiltonian matrix were obtained by fitting 214 energy levels in the bulk energy bands calculated by Burdick. The two-dimensional energy bands were calculated at 576 points in the two-dimensional Brillouin zone (2DBZ) with and without a surface-parameter shift. The planar and total densities of states are presented. Our results disagree with those of Gurman and Pendry by having surface states over a larger range of energies and by having surface states at the $\bar{M}$ point of the 2DBZ.

I. INTRODUCTION

In the only calculation of surface states for copper of which we are aware, Gurman and Pendry[1] (GP) report that surface states lie only in a narrow band of 0.08-Ry width which extends over approximately that two-thirds of the two-dimensional Brillouin zone (2DBZ) furthest from the $\bar{M}$ point. We here report a tight-binding or linear combination of atomic orbitals (LCAO) calculation of the energy bands and planar and total densities of states for a (100) copper film similar to our previous calculation for iron.[2] We find surface states lying in several absolute gaps over a much wider energy range than GP. We also find surface states at $\bar{M}$. These lie in subband gaps, i.e., in gaps in states of a particular symmetry which are filled with a continuum of states of different symmetry. As soon as one leaves the symmetry point, these surface states no longer exist and therefore even had they been found by GP, they would have contributed an amount of zero measure to their density of surface states. The quantity of physical interest is, however, not the density of surface states but the surface density of states. Since the $\bar{M}$ surface states become surface resonances off the $\bar{M}$ point, they do give an important contribution to the latter.

Other transition-metal surface calculations have either been limited to the center of the 2DBZ[3-5] or have been made with an expansion containing d orbitals only,[6,7] i.e., neglecting the important effects of s-d hybridization discussed in I.

In Sec. II, we explain the construction and diagonalization of the thin-film Hamiltonian and calculate and discuss the total (TDS) and planar (PDS) densities of states. In Sec. III we display the thin-film energy bands both without and with a surface-parameter shift and discuss the surface states appearing therein.

II. HAMILTONIAN MATRIX AND THE DENSITY OF STATES

We chose a basis set consisting of the one $4s$ function, three $4p$ functions, and five $3d$ functions. With this basis and the LCAO method of Slater and Koster,[8] we fit the bulk energy bands of Burdick[9] which were shifted upward by 0.05 Ry to get agreement with the experimental work function.[10,11] The fit was somewhat more difficult to make than for iron,[2] requiring the inclusion of third-neighbor parameters. Also, if we did not include some points on the Q line[12] in our BZ sample, we obtained unphysical values for the parameters (farther-neighbor parameters were not generally smaller than nearer-neighbor parameters). If we then added the Q-line points to our sample, the simplex minimization algorithm[13] was not able to dig itself out of the local minimum in the rms error between the calculated and Burdick's energies. Fitting the 214 energy levels below 0.191 Ry (above the vacuum level) at 39 points in the $\frac{1}{48}$th BZ (including three Q points from the beginning), we obtained the values for the 34 two-center integral parameters listed in Table I. The rms error in the fit was 6.243×10^{-3} Ry and the maximum error was 0.01775 Ry, somewhat less than we were able to obtain in I. It is interesting to note that the $dd_{(xy)0}$ and $dd_{(x^2-y^2)0}$ zero-neighbor or "atomic" parameters are almost identical as they were in iron, suggesting that the crystal-field splitting of the d levels in both fcc and bcc transition metals is negligible.

For the (100) surface of fcc copper the unit cell is a square parallelepiped extending over the thickness of the film and containing one atom in each layer. The layers alternate having one atom either at the center or corners of the unit cell. This differs from the (100) bcc unit cell only in that the square is rotated by 45° with respect to the cubic axes and is $(a/\sqrt{2})\times(a/\sqrt{2})$, where a is the cubic-unit-cell lattice parameter. In both cases the separation between layers is $\frac{1}{2}a$. Because the fcc a is larger by about a factor of $2^{1/3}$, we have chosen our film to have 33 layers, making it approximately the same thickness as the 41-layer iron film. Each layer has a separate set of nine two-dimensional (2D) Bloch basis functions yielding 297 basis functions for 33 layers. With

TABLE I. First, second, and third-neighbor Slater-Koster LCAO parameters in Ry. The last four are zero neighbors.

parameter/neighbor	1	2	3
$ss\sigma$	−0.081 304	0.007 280 7	0.000 674 66
$sp\sigma$	0.122 313	−0.002 306 9	−0.002 106 0
$sd\sigma$	−0.038 945	−0.015 865	0.000 374 9
$pp\sigma$	0.168 80	0.025 670	−0.014 890
$pp\pi$	0.001 731	0.014 460	0.000 119
$pd\sigma$	0.058 06	0.008 680	0.002 960
$pd\pi$	−0.002 273	−0.000 024 51	−0.000 809 4
$dd\sigma$	−0.026 77	−0.005 750	0.000 298 3
$dd\pi$	0.015 47	0.001 538	0.000 289 9
$dd\delta$	−0.002 064	0.000 154 1	0.000 302 3
ss_0	−0.078 363		
pp_0	0.437 10		
$dd_{(xy)0}$	−0.564 3		
$dd_{(x^2-y^2)0}$	−0.566 3		

an odd number of layers in the film, the central layer is a reflection plane which allows us to reduce the Hamiltonian matrix from 297×297 to 150 ×150 and 147×147 matrices for even and odd solutions, respectively. Using the parameters of Table I, we diagonalized the thin-film Hamiltonian at 576 points in the 2DBZ or 91 points in the $\frac{1}{8}$th irreducible wedge of the 2DBZ. Of these, 36 points are symmetry points or are on symmetry lines where the basis sets are further reduced as shown in Table II of I.

Figure 1 displays the TDS and PDS for several planes. An energy mesh of 0.001 Ry was used; each energy level was given a width of 0.005 Ry so that it contributed $\frac{1}{5}$ to the four energy intervals it overlapped completely with the remaining $\frac{1}{5}$ shared proportionally between the two intervals which were partially overlapped. The PDS is obtained by weighting the contribution of each eigenstate by the sum of the squares of the coefficients of the basis functions located on the plane of interest. The surface PDS, as expected,[2,6] has a smaller first moment than the interior PDS or the TDS. Fairly large differences extend down to the 13th layer (fourth from the surface). The four central layers are very similar but slight differences between them can be detected. The Fermi level, found by summing the TDS up to 11 electrons per atom, is at −0.3285 Ry. The number of electrons per atom on the surface layer, found by summing the surface PDS up to the Fermi energy, is 10.731. In I, we restored electrical neutrality to the iron surface plane by shifting the zeroth neighbor parameters for the surface atoms by −0.0217 Ry. To obtain electrical neutrality here we need a shift of about −0.1 Ry which is completely unphysical. This is because the Fermi energy lies well above the d-bands with their large density of states. It is a shortcoming of the restricted LCAO expansion that it cannot account for the charge that extends far beyond the crystal surface. Thus the method is not applicable to self-consistent calculations. It is, however, as accurate as any other method for non-self-consistent calculations. Furthermore, it has the advantage of being computationally simple so that one can use thicker films and perform calculations at points of no symmetry in the 2DBZ. As a parametrization scheme the lack of charge neutrality is of no consequence; given data about surface states, the surface parameters can be adjusted to fit that data. Since no such data exists, we have shifted the zeroth neighbor parameters of the surface atoms by −0.02 Ry to study the effect of such a shift on the energy bands and PDS. A dip in the potential of about half this size is found in a self-consistent calculation of lithium[14] and can be thought of as inducing the peak in the surface Friedel oscillation. Figure 2 displays the PDS and TDS in this case. The Fermi level is slightly shifted to −0.3295 Ry, the number of electrons in the surface plane is increased to 10.783 per atom. The biggest change is in the surface PDS which has been shifted by the same amount as the surface parameters. Although the width of the d bands is unchanged, the sharp peak on the high-energy edge has been suppressed and the main set of peaks lying above −0.4 Ry has been compacted. The secondary set of peaks lying below −0.4 Ry is considerably larger, due in part to surface states which have been pulled out of the bottom of the d bands.

III. ENERGY BANDS

Figure 3 shows the $\bar{\Delta}_1$-$\bar{Y}_1$-$\bar{\Sigma}_1$ and $\bar{\Delta}_2$-$\bar{Y}_2$-$\bar{\Sigma}_2$ bands as well as the $\bar{\Delta}$-$\bar{Y}$-$\bar{\Sigma}$ composite bands for the unshifted parameters. Figure 4 displays the corresponding energy bands for the shifted param-

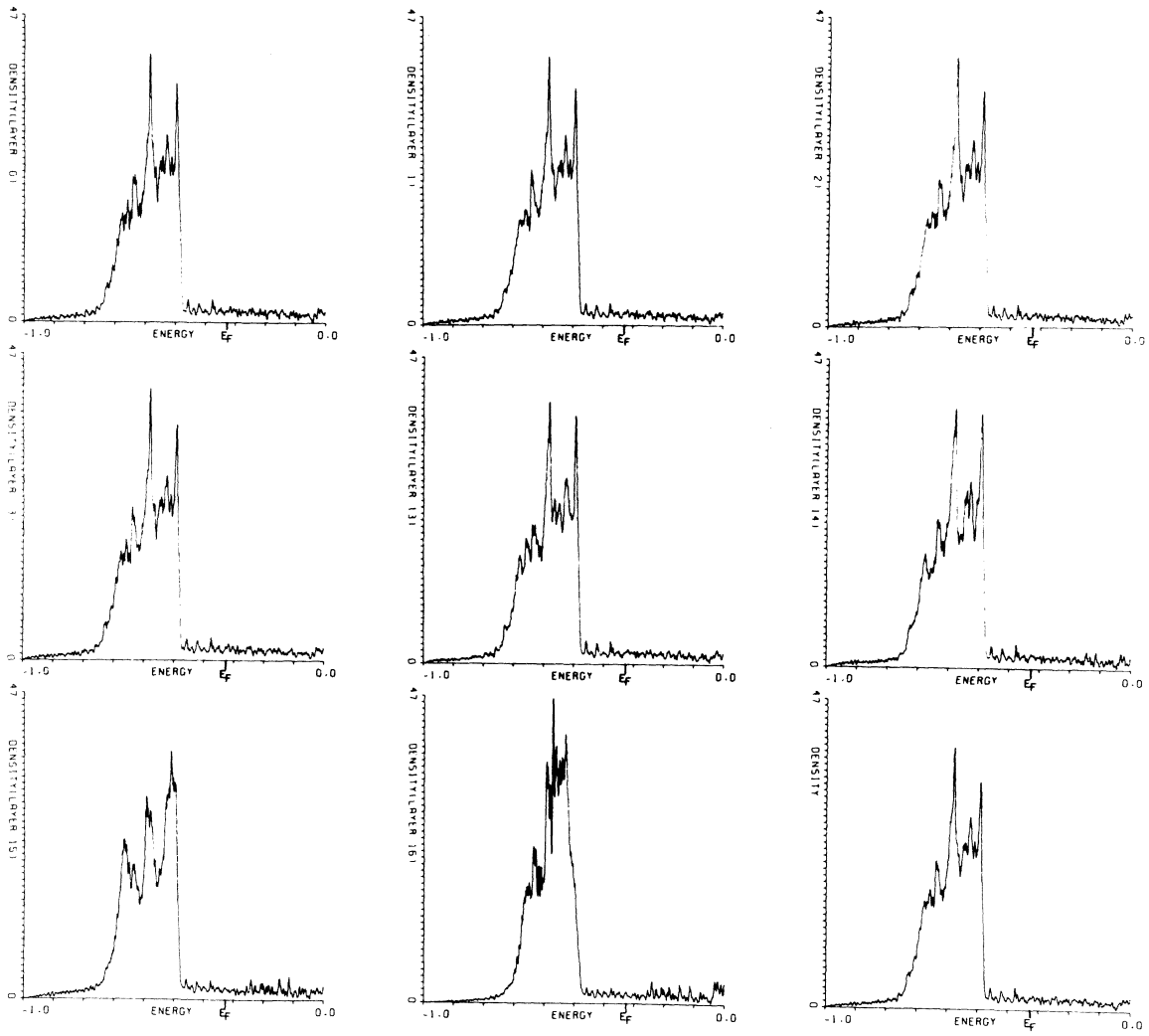

FIG. 1. Planar and total densities of states for the unshifted surface parameters. Layer 0 is the center layer and 16 is the surface layer. The units along the ordinate when multiplied by 2 for spin are electrons per atom per Ry.

eters.

For the bands with unshifted surface parameters, we have several energy gaps and surface states[15] on both high symmetry points and symmetry lines. First of all, we look at absolute gaps in the unshifted bands, i.e., gaps in the composite bands of Fig. 3, and the surface states in these absolute gaps. Along the $\bar{\Delta}$ line, i.e., $\bar{k}=(2\pi/a)(\alpha, 0)$, we have five absolute gaps, two of which have surface states. We have seven absolute gaps on the $\bar{Y}$ line, i.e., $(2\pi/a)(\frac{1}{2}, \alpha)$ six of which have surface states, and three absolute gaps on the $\bar{\Sigma}$ $[\bar{k}=(2\pi/a)(\alpha, \alpha)]$ line, one of which has a surface state.

The first gap on the $\bar{\Delta}$ and $\bar{\Sigma}$ lines starts on $\bar{\Gamma}$ at approximately -0.18 Ry and continues up above the vacuum level, extending $\frac{7}{12}$ of the way to $\bar{X}$ and $\frac{5}{12}$ of the way to $\bar{M}$. It has no surface state. The second gap in the $\bar{\Delta}$ line and the first gap on the $\bar{Y}$ line starts on $\bar{X}$ at approximately -0.38 Ry and extends $\frac{5}{12}$ of the way to $\bar{\Gamma}$ and $\frac{9}{12}$ of the way to $\bar{M}$. In this gap we have two surface states; the upper surface state, starting on $\bar{X}$ at -0.035 Ry, has either $\bar{\Delta}_1$ symmetry or $\bar{Y}_1$ symmetry and $\bar{X}_1$ symmetry on $\bar{X}$, and runs along the top of the gap. The lower one having $\bar{X}_3$ symmetry on $\bar{X}$ at -0.257 Ry has either $\bar{\Delta}_1$ or $\bar{Y}_2$ symmetry and runs the entire length of the gap.

The second $\bar{Y}$ gap runs the entire length of $\bar{Y}$, connecting to the second gap on $\bar{\Sigma}$, closing off $\frac{4}{12}$ of the way from $\bar{M}$ to $\bar{\Gamma}$, and to the third gap on $\bar{\Delta}$ closing off $\frac{5}{24}$ of the way from $\bar{X}$ to $\bar{\Gamma}$. There is no surface state in this gap. The fourth $\bar{\Delta}$ gap at about -0.6 Ry runs between points lying approximately $\frac{2}{12}$ and $\frac{7}{12}$ of the distance between $\bar{\Gamma}$ and $\bar{X}$. In this gap we have no surface state. The fifth and last gap on $\bar{\Delta}$ runs the entire length of $\bar{\Delta}$, connecting on one side to the seventh $\bar{Y}$ gap and on the other side to the third $\bar{\Sigma}$ gap. This extensive en-

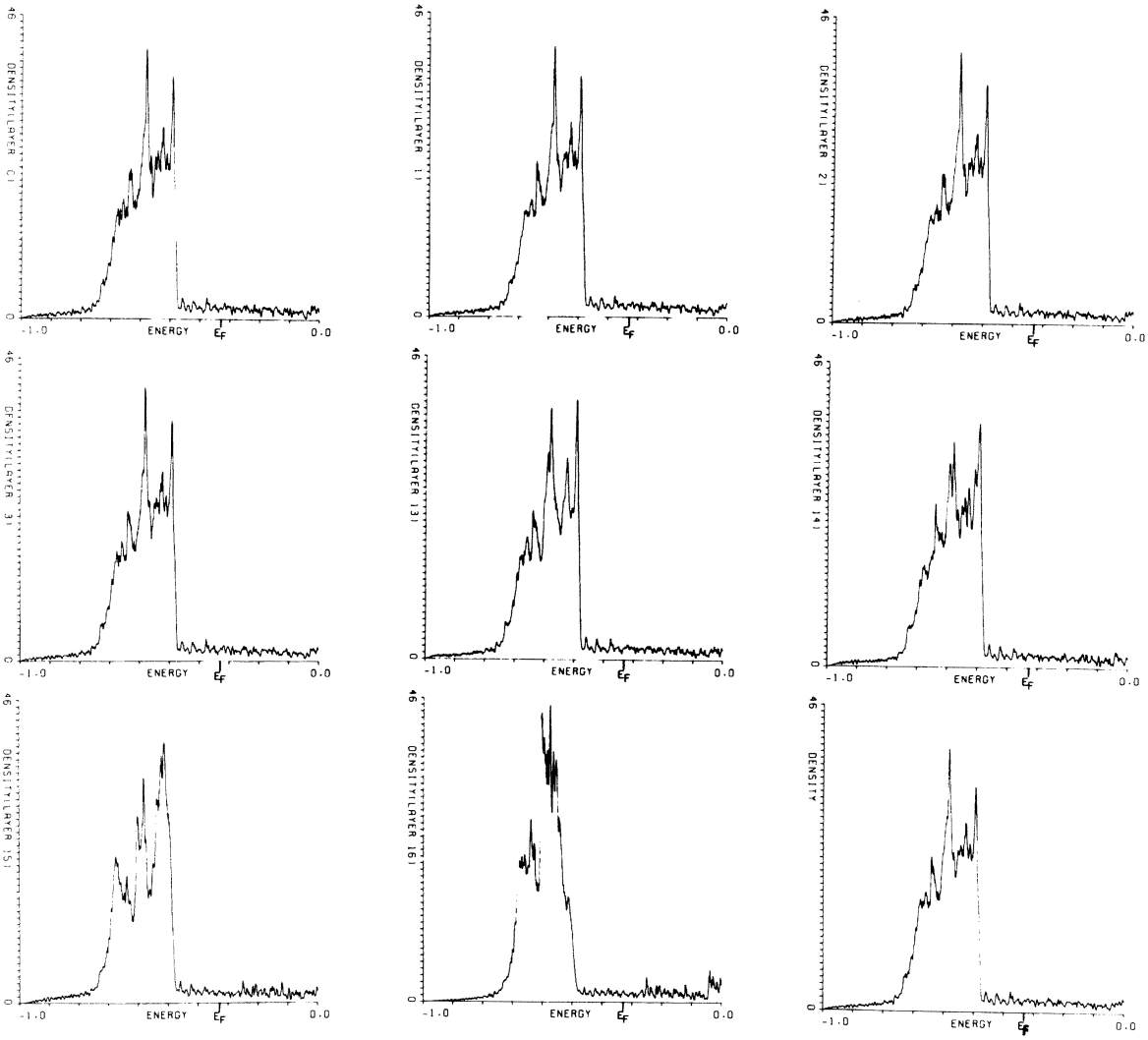

FIG. 2. Planar and total densities of states for the shifted surface parameters. The units along the ordinate when multiplied by 2 for spin are electrons per atom per Ry.

ergy gap closes off along $\bar{Y}$ $\frac{4}{12}$ of the way between $\bar{X}$ and $\bar{M}$ and along $\bar{\Sigma}$ $\frac{3}{12}$ of the way to $\bar{M}$ from $\bar{\Gamma}$. A $\bar{\Gamma}_1$ surface state at -0.699 Ry continues as a $\bar{\Delta}_1$ surface state which runs along the top of this gap $\frac{4}{12}$ of the way to $\bar{X}$ where it peels off and runs through the gap $\frac{7}{12}$ of the way to $\bar{X}$. At this point, it runs along the bottom of the gap as either a resonance or a surface state with a decay length of the order of the film thickness. Then, $\frac{10}{12}$ of the way to $\bar{X}$, it peels off the bottom of the gap and runs as a surface state into the $\bar{X}_1$ surface state at -0.664 Ry. A $\bar{Y}_1$ surface state runs from the $\bar{X}_1$, the length of the $\bar{Y}$ gap. A $\bar{\Sigma}_1$ branch of this surface state runs along the top of the absolute $\bar{\Sigma}$ gap but is actually running near the bottom of a much wider and longer $\bar{\Sigma}_1$ subband gap $\frac{8}{12}$ of the way to $\bar{M}$. This extensive surface state appears to be one found by GP.

The third $\bar{Y}$ gap at -0.5 Ry is very thin and extends from $\frac{2}{12}$ to $\frac{11}{12}$ of the way to $\bar{M}$ from $\bar{X}$. It contains two pairs of surface states which run its entire length. The upper pair has $\bar{Y}_2$ symmetry and the lower pair has $\bar{Y}_1$. Each pair is slightly split because the long decay length causes overlap of the states on the two surfaces destroying the degeneracy of the pair. In fact, if these states did not lie well within the gap they could not be distinguished from resonances. These surface states lie outside the energy range in which GP found surface states. The fourth $\bar{Y}$ gap is very narrow. It starts at $\bar{X}$ where it is pinched off at -0.57 Ry. It pinches off $\frac{5}{12}$ of the way to $\bar{M}$ but then continues on to $\frac{7}{12}$ of the way to $\bar{M}$ where it pinches off again. To the right of the $\frac{5}{12}$ pinch it contains a $\bar{Y}_1$ surface

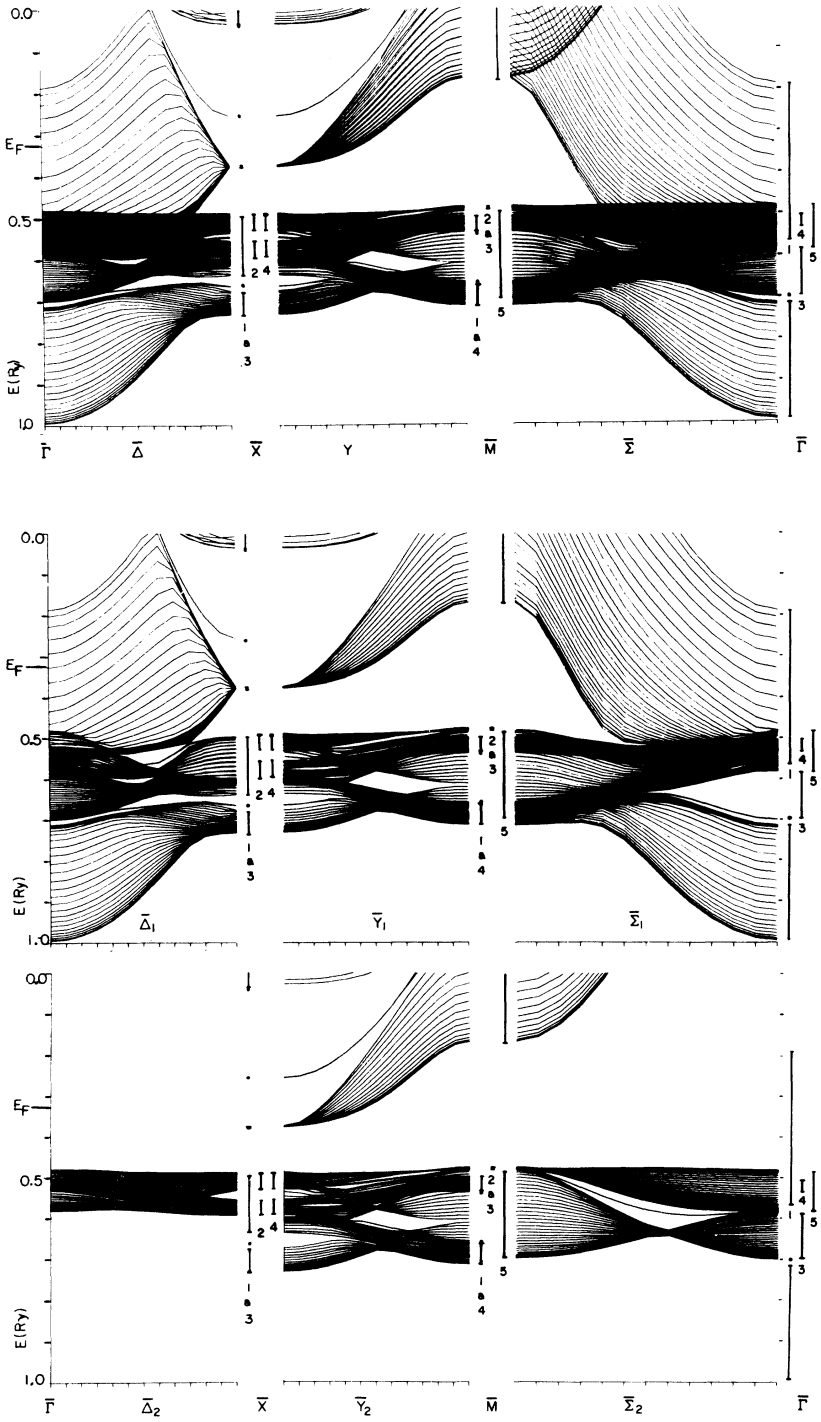

FIG. 3. Two-dimensional energy bands for unshifted surface parameters.

state and to the left a $\bar{Y}_2$. This gap is most easily seen by looking at the $\bar{Y}_1$ and $\bar{Y}_2$ bands in the regions in which the gap is not obscured by the surface state. The fifth gap is a large parallelepiped at about -0.6 Ry which runs between $\frac{4}{12}$ of the way to $\bar{M}$ and $\bar{M}$ where it pinches off. It contains a $\bar{Y}_2$ surface state running above its bottom to $\frac{8}{12}$ of the way to $\bar{M}$. The sixth gap runs from $\frac{2}{12}$ to $\frac{5}{12}$ of the way to $\bar{M}$. It is located just above and to the left of the parallelepiped. It is very narrow, contains a $\bar{Y}_2$ surface state between $\frac{2}{12}$ and $\frac{4}{12}$, and is most easily observed in the $\bar{Y}_1$ bands. None of these Y gaps extend very far off the $\bar{Y}$ line. There are two apparent $\bar{Y}$ gaps which start at $\bar{X}$, a wide one at

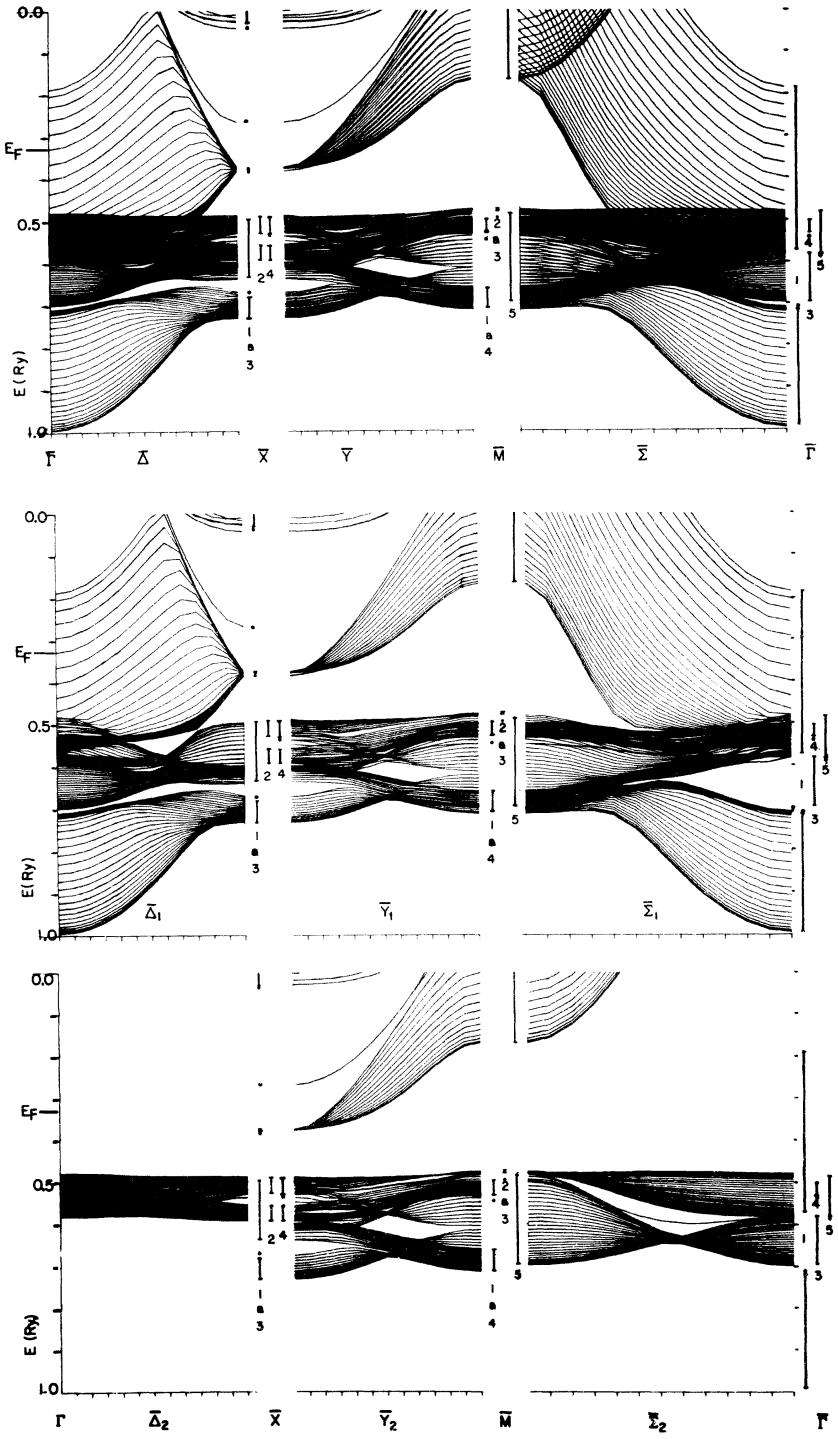

FIG. 4. Two-dimensional energy bands for shifted surface parameters.

– 0.54 Ry and a narrow one at – 0.595 Ry. These are, however, filled with a continuum of states whose density is not as great as in surrounding regions. In a thicker film they would not appear to be gaps.

We now look at subband gaps, i.e., gaps in bands of one symmetry which are overlapped by bands of another symmetry. We have two $\bar{M}$ surface states, an $\bar{M}_1$ at – 0.535 Ry and an $\bar{M}_4$ at – 0.656 Ry. The $\bar{M}_1$ surface state decays into $\bar{Y}_1$ and $\bar{\Sigma}_1$ resonances, which exist $\frac{2}{12}$ of the way to $\bar{X}$, and $\frac{3}{12}$ of the way to $\bar{\Gamma}$. The $\bar{M}_4$ surface state decays into $\bar{Y}_2$ and $\bar{\Sigma}_1$ resonances which exist $\frac{2}{12}$ of the way to $\bar{X}$ and $\bar{\Gamma}$. The third absolute $\bar{\Delta}$ gap starts

at $\bar{X}$ at -0.4 Ry and is pinched off by $\bar{\Delta}_2$ states $\frac{5}{24}$ of the way to $\bar{\Gamma}$. It continues as a $\bar{\Delta}_1$ subband gap, pinches off and reopens $\frac{3}{12}$ of the way to $\bar{\Gamma}$. It finally pinches off again $\frac{8}{12}$ of the way to $\bar{\Gamma}$. Between the $\frac{3}{12}$ pinch and $\frac{6}{12}$ of the way to $\bar{\Gamma}$ it contains a $\bar{\Delta}_1$ surface state. There is a $\bar{\Delta}_2$ subband gap containing no surface states starting at $\bar{X}$ at -0.54 Ry and closing $\frac{3}{12}$ of the way to $\bar{\Gamma}$. There are no $\bar{Y}$ subband gaps since $\bar{Y}_1$ and $\bar{Y}_2$ states are degenerate in the bulk and (except for surface states) essentially degenerate in a 33-layer film. The second absolute $\bar{\Sigma}$ gap has a small $\bar{\Sigma}_1$ subband gap extension at -0.48 Ry and contains no surface states. The third absolute $\bar{\Sigma}$ gap is engulfed by a much larger $\bar{\Sigma}_1$ subband gap. The $\bar{\Sigma}_1$ surface state starting from a $\bar{\Gamma}_1$ surface state, which lies at the top of the absolute gap, lies close to the bottom of the $\bar{\Sigma}_1$ subband gap and extends $\frac{8}{12}$ of the way to $\bar{M}$. There is a $\bar{\Sigma}_2$ subband gap, running from $\bar{\Gamma}$ to $\bar{M}$ but pinched off at both ends, which contains a $\bar{\Sigma}_2$ surface state over its entire length. This connects through an $\bar{M}_3$ resonance to a $\bar{Y}_2$ surface state already discussed.

There is one more feature of these bands worth mentioning. There is a band of $\bar{X}_1$ and $\bar{X}_3$ bulk states at -0.375 Ry which is only 0.003 Ry wide. This band is projected from a 3D band running from the L_2' state at $(2\pi/a)$ $(\frac{1}{2}, \frac{1}{2}, \frac{1}{2})$ to the $\bar{\Sigma}_1$ state at $(2\pi/a)$ $(\frac{1}{2}, \frac{1}{2}, 0)$. This s-p band has the very narrow width of 0.012 Ry. The reduction from 0.012 to 0.003 Ry appears to be a thin-film effect. Although thin film effects much larger than this in magnitude are quite common, we have never noticed one so large in percentage. A similar thing happens to the $\bar{M}_2$, $\bar{M}_3$ band at -0.48 Ry. It is projected from a band of 0.0042-Ry width[16] and is reduced to 0.0023-Ry width in the 33-layer film.

Turning to the bands in Fig. 4 with the surface parameter shift, we find no significant differences from Fig. 3 except for the appearance and disappearance of surface states. Two new surface states appear at $\bar{X}$. They are an $\bar{X}_1$ at -0.384 Ry and an $\bar{X}_4$ at -0.54 Ry. The $\bar{X}_1$ extends with $\bar{\Delta}_1$ and $\bar{Y}_1$ symmetry $\frac{1}{12}$ of the way to $\bar{\Gamma}$ and $\frac{3}{12}$ of the way to $\bar{M}$ along the top of the large absolute gap. The $\bar{X}_4$ continues as a $\bar{\Delta}_2$ surface state for the entire length of the subband gap. Two new $\bar{\Delta}_1$ surface states appear in the fourth absolute $\bar{\Delta}$ gap. The upper one lies right along the top of the gap and cannot be distinguished in the figure. There is a $\bar{\Delta}_2$ surface state pulled out of the bottom of the $\bar{\Delta}_2$ band which runs from $\bar{\Gamma}$ to $\frac{8}{12}$ of the way to $\bar{X}$. It lies too close to the bottom of the band to be distinguished in Fig. 4. It joins the new $\bar{\Gamma}_5$ surface state and continues as a $\bar{\Sigma}_1$ surface state in the $\bar{\Sigma}_1$ subband gap. The $\bar{\Sigma}_1$ surface state can be observed in Fig. 4 and runs along the top of the gap $\frac{5}{24}$ of the way to $\bar{M}$.

The fourth $\bar{Y}$ gap has lost the $\bar{Y}_1$ surface state it had to the right of the pinch but retains the $\bar{Y}_2$ surface state to the left of the pinch. The $\bar{Y}_2$ surface state has been pulled out of the parallelepiped-shaped gap and two $\bar{Y}_1$ surface states have been pulled into the top of the gap to replace it. A $\bar{\Delta}_1$ surface state previously ran from a $\bar{\Gamma}_1$ surface state along the top of the lowest $\bar{\Delta}$ gap $\frac{4}{12}$ of the way to $\bar{X}$ where it peeled off and ran through the center of the gap. It now runs along the bottom of the gap (perhaps as a strong resonance rather than a surface state) to the $\frac{4}{12}$ point where it disappears. The $\bar{X}_3$ surface state and its continuation as a $\bar{\Delta}_1$ surface state near the bottom of the same gap have been pulled down and had their decay length increased so that one cannot tell if they are still surface states at the bottom of the gap or are resonances at the top of the continuum. A new $\bar{\Sigma}_2$ surface state is pushed out of the bottom of the lowest $\bar{\Sigma}_2$ band where it has a kink $\frac{5}{12}$ of the way to $\bar{M}$ from $\bar{\Gamma}$. Other effects of the surface parameter shift are the pushing down of an $\bar{M}_3$ surface state at -0.498 Ry from the bottom of the lowest $\bar{M}_3$ band and the disappearance of the $\bar{M}_4$ surface state into the top of the lowest $\bar{M}_4$ band. The new $\bar{M}_3$ surface state decays into resonance states upon leaving $\bar{M}$ as does a new $\bar{\Gamma}_4$ surface state at -0.542 Ry upon leaving $\bar{\Gamma}$.

In conclusion, as for iron, we have found energy gaps throughout the 2DBZ, some of which contain surface states and some of which do not. The occurence of surface states in the various gaps is somewhat more sensitive to the surface parameters than it was in iron because the energy gaps of copper are narrower. Although we found resonances connecting to subband gap surface states and some isolated resonances, we did not find resonances extending throughout the 2DBZ as we did in iron.

---

*Supported by National Science Foundation Grant No. DMR 73-02449-A01.

[1]S. J. Gurman and J. B. Pendry, Phys. Rev. Lett. 31, 637 (1973); hereafter called GP.

[2]D. G. Dempsey, L. Kleinman, and Ed Caruthers, Phys. Rev. B 12, 2932 (1975); hereafter called I.

[3]R. V. Kasowski, Phys. Rev. Lett. 33, 83 (1974); the film in this copper calculation was too thin to find the surface state.

[4]E. Caruthers and L. Kleinman, Phys. Rev. Lett. 35, 738 (1975).

[5]R. V. Kasowski, Solid State Commun. 17, 179 (1975).

[6]M. C. Desjonqueres and F. Cyrot-Lackmann, J. Phys. Lett. (Paris) 36, L45 (1975); J. Phys. F 5, 1368 (1975).

[7]R. Haydock, V. Heine, and M. J. Kelly, J. Phys. C 5, 2845 (1972); and R. Haydock and M. J. Kelly, Surf. Sci. 38, 139 (1973).

[8]J. C. Slater and G. F. Koster, Phys. Rev. 94, 1498 (1954).
[9]G. A. Burdick, Phys. Rev. 129, 138 (1963).
[10]S. C. Jain and K. S. Krishman, Proc. R. Soc. A 210, 170 (1952).
[11]J. E. Rowe and N. V. Smith, Phys. Rev. B 10, 3207 (1974).
[12]This line lies on the hexagonal face of the BZ between $(2\pi/a)$ $(\frac{1}{2},\frac{1}{2},\frac{1}{2})$ and $(2\pi/a)$ $(1,\frac{1}{2},0)$.
[13]J. A. Nelder and R. Mead, Comput. J. 7, 308 (1965).
[14]G. P. Alldredge and L. Kleinman, Phys. Rev. B 10, 559 (1974).
[15]By surface state we mean pair of degenerate surface states, one on each surface of the film. If the decay length is sufficiently long that they overlap, the degeneracy is broken and the eigenstates are even and odd combinations of the pair.
[16]This $X_5 - Z_2 - W_1'$ band is actually of zero width to three significant figures in Burdick's calculation! But in our LCAO fit to Burdick's calculation it acquired the stated width.

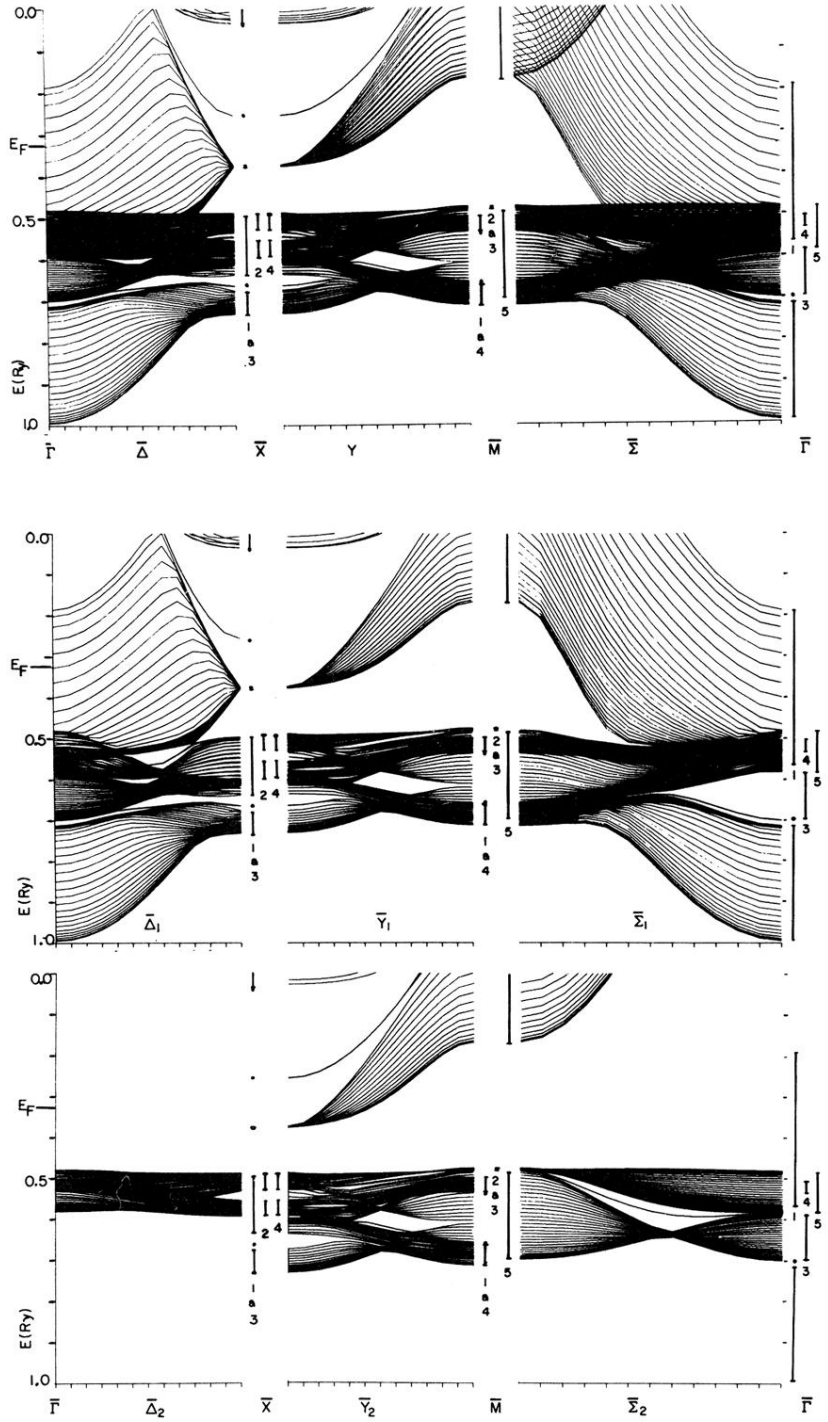

FIG. 3. Two-dimensional energy bands for unshifted surface parameters.

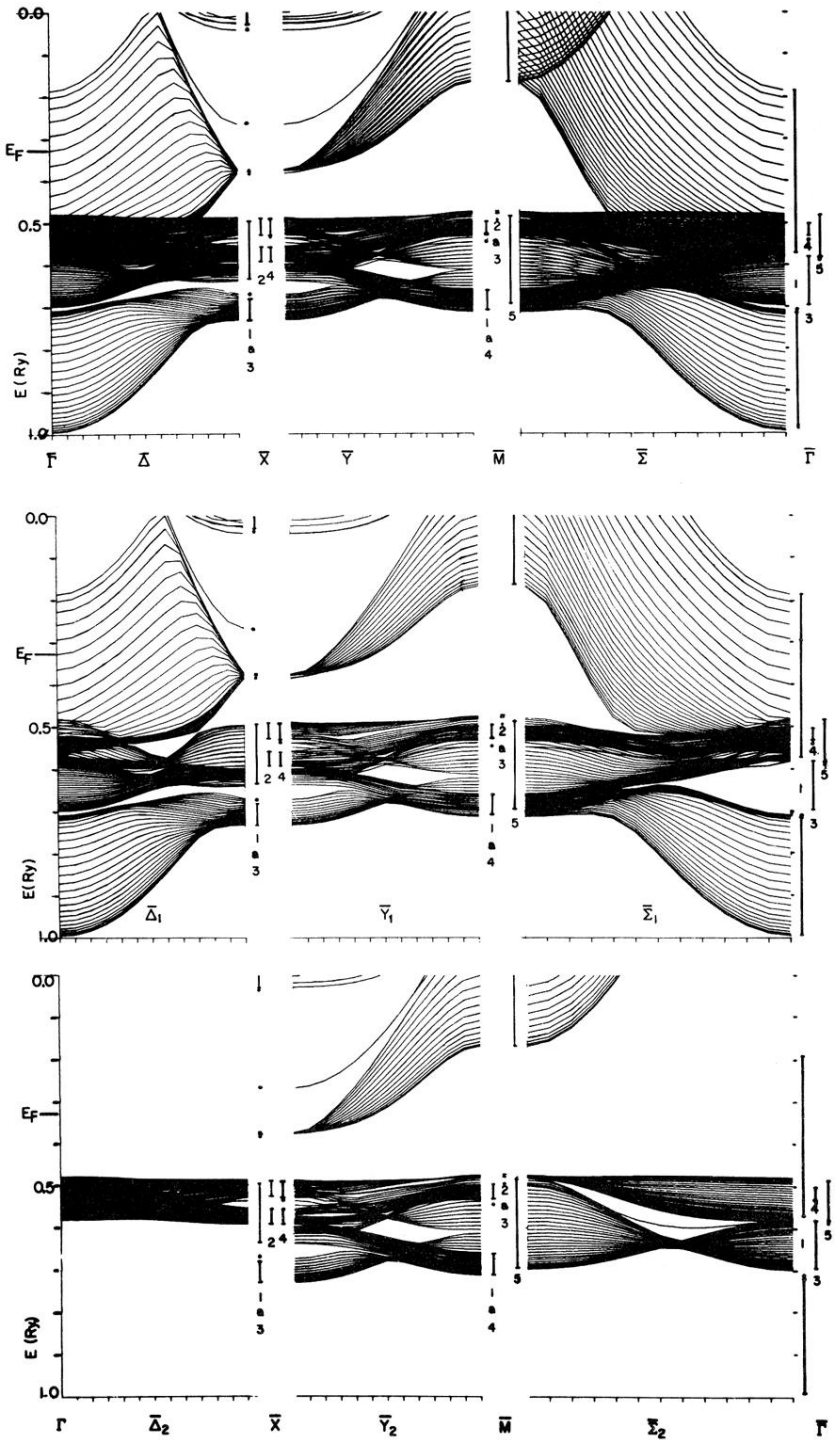

FIG. 4. Two-dimensional energy bands for shifted surface parameters.